Geophysical Journal International

Geophys. J. Int. (2010) **183,** 103–110 doi: 10.1111/j.1365-246X.2010.04747.x

Energetic rupture, coseismic and post-seismic response of the 2008 M_W 6.4 Achaia-Elia Earthquake in northwestern Peloponnese, Greece: an indicator of an immature transform fault zone

Lujia Feng,[1] Andrew V. Newman,[1] Grant T. Farmer,[1]* Panos Psimoulis[2] and Stathis C. Stiros[2]

[1]*School of Earth and Atmospheric Sciences, Georgia Institute of Technology,* 311 *Ferst Drive, Atlanta, GA* 30332*, USA. E-mail: anewman@gatech.edu*
[2]*Department of Civil Engineering, University of Patras, Patras* 26500*, Greece*

Accepted 2010 July 19. Received 2010 July 19; in original form 2009 December 9

SUMMARY

The 2008 June 8, moment magnitude M_W 6.4 crustal earthquake in northwestern Peloponnese, Greece, was a strong-shaking dextral strike-slip event with teleseismic broad-band and high-frequency energy magnitudes M_e of 6.8 and 7.2, respectively. A high stress drop 5–10 times the global average is associated with excessive high-frequency energy. The NE–SW trending fault plane shown by the aftershock distribution and focal mechanism is not associated with previously mapped faults, and no obvious coseismic surface rupture was discovered. Contrasting the enhanced rupture energy, the event created no substantial coseismic or post-seismic surface deformation, likely due to a fault buried below a detached thick and compositionally weak flysch layer. Comparative spatial analysis including over 30 regional strike-slip events between 1965 and 2009 reveals a NE–SW striking diffuse transform fault zone subparallel to the Cephalonia Transform Fault. The dextral sense of motion along the transform zone is consistent with the ongoing Global Positioning System (GPS)-derived deformation along the West Hellenic Arc and the motion on the Cephalonia Transform Fault. Characterizing this system is important to constraining the seismic hazard near Patras, a major port city immediately NE of the 2008 event.

Key words: Satellite geodesy; Radar interferometry; Seismicity and tectonics; Transform faults; Dynamics and mechanics of faulting; Europe.

INTRODUCTION

On 2008 June 8, a strong rupturing crustal earthquake struck NW Peloponnese, Greece (Fig. 1b). The event is reported as a moment magnitude $M_W = 6.4$ strike-slip earthquake by the global centroid moment tensor (gCMT) catalogue (Eskröm *et al.* 2005), making it the largest such event instrumentally recorded in this area. The enhanced shaking of this earthquake was felt throughout mainland Greece. It triggered a number of landslides and rockfalls, toppled old buildings and un-/poorly reinforced houses and cracked reinforced concrete building in nearby communities. Secondary ground fissures were observed on the pavement of roads and bridges; however, neither positive evidence of surface rupture nor significant surface deformation was observed (Briole *et al.* 2008; Ganas *et al.* 2009; Margaris *et al.* 2010; this study).

The Peloponnese is part of the Aegean microplate, which is fast moving to the SW away from Eurasia at ∼30 mm yr^{-1} (McClusky *et al.* 2000; Reilinger *et al.* 2006), overriding the African Plate along the Hellenic subduction zone to the south at ∼5 mm yr^{-1} (McClusky *et al.* 2000; Fernandes *et al.* 2003) and sliding past the Apulian platform along the dextral strike-slip Cephalonia Transform Fault (CTF) to the west (e.g. van Hinsbergen *et al.* 2006, Fig. 1a). Global Positioning System (GPS) sites east of the CTF show increased relative motion southward from ∼10 mm yr^{-1} to ∼30 mm yr^{-1} (Hollenstein *et al.* 2006, 2008). Aegean–Eurasian motion is partially localized on WNW–ESE trending normal faults within the fast-spreading young rift forming the Gulf of Corinth (GC, Fig. 1a). N–S extension within the rift increases from 11 mm yr^{-1} in the central zone to 16 mm yr^{-1} in the west (Avallone *et al.* 2004). To first order, the Peloponnese is considered to move along with the Aegean Plate with little internal deformation (<2 mm yr^{-1}; McClusky *et al.* 2000); however, motion in the NW Peloponnese is modestly reduced and perturbed toward the south (Hollenstein *et al.* 2008 and fig. 6 therein). Le Pichon *et al.* (1995) proposed that the NW Peloponnese belongs to the central Ionian Islands block rather than the Peloponnese system. Due to lack

*Now at: School of Earth, Atmospheric and Planetary Sciences, Massachusetts Institute of Technology, 77 Massachusetts Ave., Cambridge, MA 02139-4307, USA.

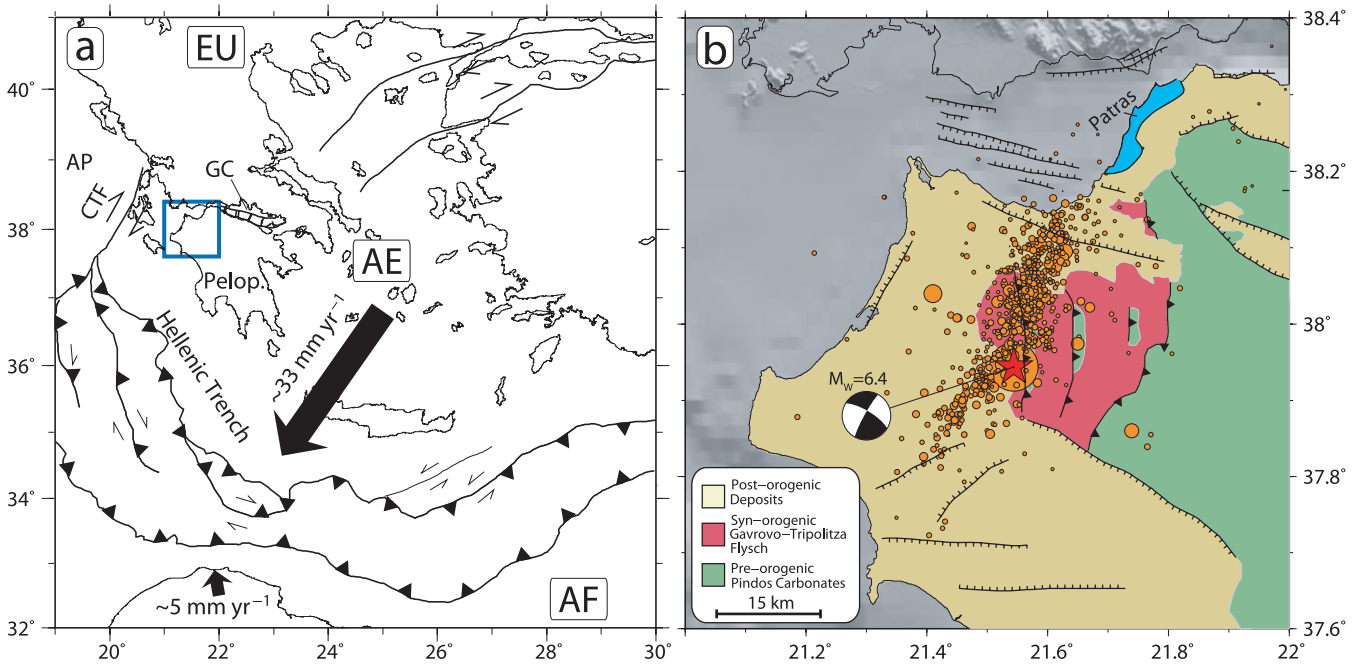

Figure 1. (a) Regional tectonic map of the Aegean. The major boundaries are simplified after Kreemer & Chamot-Rooke (2004). Arrows show the relative motion of the Aegean (AE) (Reilinger *et al.* 2006; Ganas & Parsons 2009) and African (AF) (Fernandes *et al.* 2003; Ganas & Parsons 2009) Plates to Eurasia (EU). Pelop., Peloponnese; GC, Gulf of Corinth; AP, Apulian Platform; CTF, Cephalonia Transform Fault. Solid blue box outlines the region of Fig. 1(b). (b) Simplified geological map of NW Peloponnese. Normal faults are combined from Doutsos & Kokkalas (2001) and Flotté *et al.* (2005). Thrust faults are adapted from van Hinsbergen *et al.* (2006). Orange circles indicate the 2008 June 8, main shock and 10-d aftershocks taken from the preliminary seismic catalogue of Aristotle University of Thessaloniki (AUTh catalogue) (http://geophysics.geo.auth.gr/index_en.html). Red star is the mainshock epicentre representing rupture initiation. The gCMT focal mechanism for the main shock is consistent with other reporting institutions. The earthquake does not associate with any existing mapped fault. The populated Patras metropolitan area is highlighted in turquoise.

of sufficient modern geodetic observations and low-rate seismicity, the extent and accommodation of strain across the region remained unclear before the 2008 Achaia-Elia Earthquake.

The 2008 Achaia-Elia Earthquake exhibits an approximately 25 km long NE–SW trending aftershock distribution that, together with fault plane solutions (compiled in Ganas *et al.* 2009), clearly indicates right-lateral strike-slip on a near-vertically dipping fault that is unassociated with existing mapped faults (Fig. 1b). The earliest identified fault system in the NW Peloponnese is the N–S to NNW–SSE striking thrusts with secondary sinistral WNW–ESE and dextral WSW–ENE strike-slip faults (Kamberis *et al.* 2000) active from the late Eocene to the Oligocene (Sotiropoulos *et al.* 2003; van Hinsbergen *et al.* 2005) as a part of the west-verging External Hellenide orogenic belt. The active thrust front has moved westwards to the West Hellenic Arc as shown by the destructive surface wave magnitude $M_s = 7.2$ Cephalonia earthquake in 1953 (Stiros *et al.* 1994). After the collisional episode, two independent and locally interacting sets of WNW–ESE and NE–SW trending normal faults related to the latest extensional stage dominated the area since the late Pliocene (Doutsos & Kokkalas 2001). The 2008 earthquake does not correspond to, but instead crosscuts the pre-existing thrusts and normal faults. We show the NE–SW trending strike-slip faulting of the 2008 June 8, earthquake is likely part of an early stage of a diffuse transform regime, accommodating dextral motion between the Apulian and Aegean plates along with the CTF (Fig. 1a). Because Patras, the third largest city in Greece, is located only ~35 km from the epicentre and is in the approximate striking plane of the 2008 earthquake, the continued activity along this transform system poses a previously poorly understood seismic hazard.

STRONG RUPTURE

Using the methodology and algorithms of Newman & Okal (1998) and Newman & Convers (2010), we evaluate the radiated seismic energy from teleseismically distributed (between 25° and 80° from the event) broad-band vertical waveforms. Averaging the seismic energy as determined from 53 stations after correcting for distance, attenuation, focal mechanism and depth, we find that the 2008 Achaia-Elia Earthquake had excessive rupture energy that may have contributed to the enhanced shaking that caused regional damage. We obtain broad-band (period 0.5 s to 70 s) energy $E_{bb} = 4 \times 10^{14}$ J and high-frequency (period 0.5 s to 2 s) energy $E_{hf} = 2.7 \times 10^{14}$ J that correspond to broad-band and high-frequency energy magnitudes $M_{e\text{-}bb} = 6.8$ and $M_{e\text{-}hf} = 7.2$, respectively, using the conversion from Choy & Boatwright (1995):

$$M_{e\text{-}bb} = 2/3 \, \mathrm{Log}_{10}(E_{bb}) - 2.9, \quad (1)$$

after making a standard conversion from E_{hf} to E_{bb} using the relationship $E_{bb} = 5E_{hf}$ from Newman & Convers (2010). Our determinations are similar to the reported energy magnitude $M_e = 7.0$ from the US Geological Survey Preliminary Determinations of Epicentres (catalogue described in Dewey *et al.* 2007). The 0.4 and 0.8 unit magnitude discrepancies between the energy and moment magnitudes highlight the disproportional increase in high-frequency shaking of the event, which may be the result of relatively high stress drop $\Delta\sigma$.

Such a determination can be made by the direct comparison between energy E_{bb} and moment release M_0 of an event, where

$$\Delta\sigma = 2GE_{bb}/M_0, \quad (2)$$

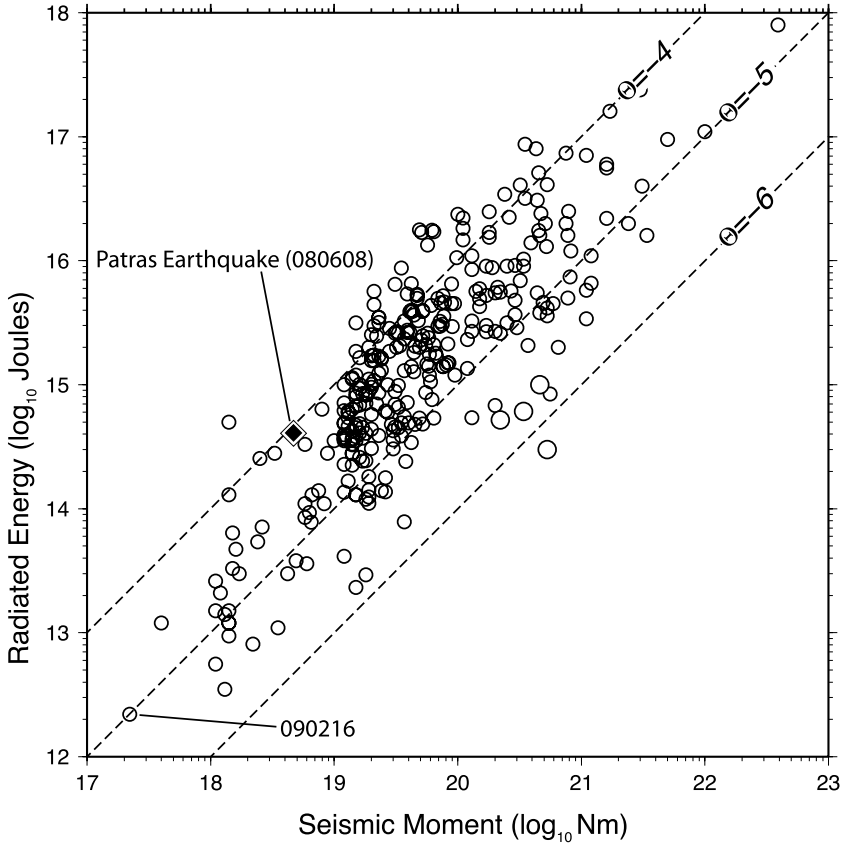

Figure 2. Distribution of radiated broad-band seismic energy to moment showing the relationship for most earthquakes (open circles) is near $E_{bb}/M_0 = 10^{-4.8}$ (figure after Newman & Convers 2010). The Patras event (filled diamond) is anomalously high in energy, with $E_{bb}/M_0 = 10^{-4.1}$, which can be explained by excessive $\Delta\sigma$, while a smaller M_W 5.5 event (090216) approximately 50 km away maintains an energy ratio similar to the global average.

allowing few assumptions about the extent of coseismic and final stress along the rupture and regional crustal rigidity G (e.g. Stein & Wysession 2003). The energy to moment ratios E_{bb}/M_0 for large global events range between $10^{-4.8}$ and $10^{-5.0}$ (Choy & Boatwright 1995; Newman & Okal 1998; Weinstein & Okal 2005), which yields $\Delta\sigma$ estimates between 0.6 and 1 MPa assuming $G = 30$ GPa. Using the same conversion for the 2008 Achaia-Elia Earthquake, where $E_{bb}/M_0 = 10^{-4.1}$ (Fig. 2), we find $\Delta\sigma = 5$ MPa, a value that is between 5 and 10 times the global average. A nearby event (090 216 in Fig. 2) has $\Delta\sigma = 0.6$ MPa, comparable to the global average, suggesting that the large stress-drop associate with the Achaia-Elia Earthquake is not due to regional changes in rigidity. (Herein, event identifiers represent the date of the event: YYMMDD). Explanations of such a high $\Delta\sigma$ include a relatively large or fast coseismic slip, which may be due to rupture of an immature fault containing little, if any, fault gouge (Marone 1998).

It should be noted that the observed stress drop for this event is not significantly larger (less than a factor of 2) than the independently determined global average $\Delta\sigma = 3$ MPa from another global study that estimated results using precision determination of corner frequencies (Allmann & Shearer 2009). Though a direct comparison of average stress drops between this study and those of Allmann & Shearer (2009) cannot be made because of differences in methods, their findings of near an order of magnitude variance and a factor of two or more increase in $\Delta\sigma$ of strike-slip events is intriguing.

InSAR COSEISMIC ANALYSIS

To explore the possible spatial extent of coseismic surface displacement, we utilized repeat passes of C-band ENVISAT (European Space Agency satellite) Synthetic Aperture Radar (SAR) phase data encompassing the coseismic period to construct Interferometric SAR (InSAR) images using ROI_PAC software (Rosen *et al.* 2004). Since the satellite's right-looking ascending (northward) path is advantageous for detecting NE–SW motion, ascending scenes on 2007 December 16 and 2008 July 13 (Fig. 4a) are expected to be optimal, however, are largely decorrelated in the zone of interest. A second descending orbit pair was also examined with comparable areas of decorrelation. Unfortunately, in either image, little substantive information about the coseismic displacement could be obtained. However, regions near the projected fault plane maintain modest coherence in the ascending image, yet little interference consistent with coseismic activity is identifiable, implying buried and perhaps detached slip in the subsurface.

GPS POST-SEISMIC ANALYSIS

To record possible post-seismic surface deformation, a local network of nine continuous GPS sites was rapidly deployed between 24 and 72 hr of the initial rupture, and maintained for approximately six weeks (Fig. 3a). The sites including one base station at the University of Patras, and eight stations near the early aftershock

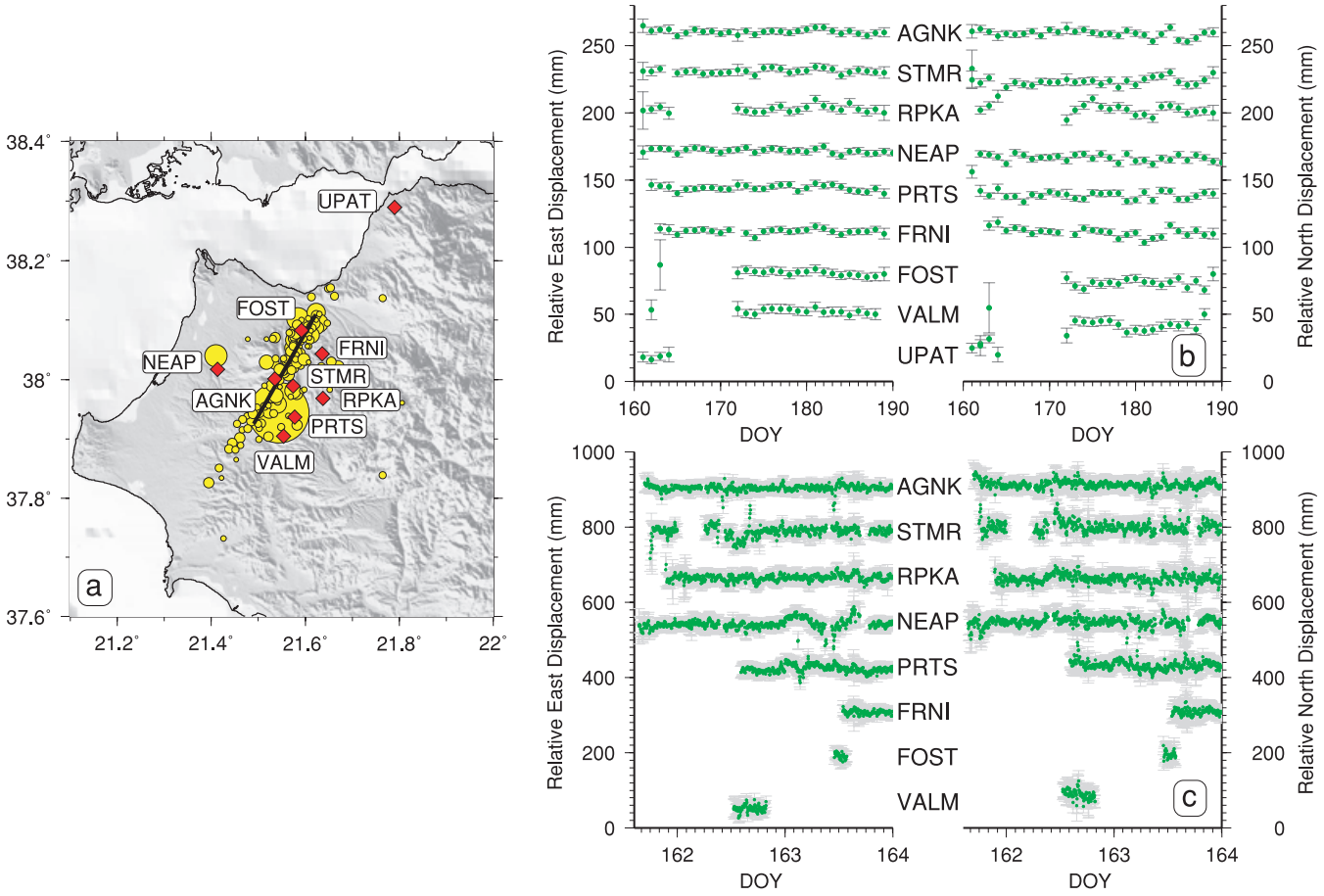

Figure 3. (a) Location of the temporary network of nine continuous GPS sites (red diamonds). Thick solid line striking N30°E defined by the southern end [21.490°, 37.925°] and the northern end [21.633°, 38.120°] represents the approximately 25-km long projected fault trace estimated from main shock and 1 d of aftershocks (yellow circles; AUTh catalogue). (b) JPL-GIPSY daily solutions for post-seismic period. (c) GAMIT-Track solutions for the first 3 d of recording. Data are 5-min averaged 15-s kinematic solutions relative to site UPAT. Neither daily (b) nor rapid kinematic solutions (c) show discernible post-seismic displacement across the network.

locations. Sites were installed either on rooftops of visibly undamaged 1–2 story homes, or on exposed bedrock in open fields. Six weeks of daily point-position solutions were determined using JPL-GIPSY (Zumberge *et al.* 1997). For the initial 3 d, 15-s kinematic solutions relative to site UPAT were determined using the Track software included with GAMIT/GLOBK (Herring *et al.* 2008). Even though numerous M_L 2–4 aftershocks continued in this region (Ganas *et al.* 2009), no discernible early post-seismic deformation was identified across the network using either daily solutions or rapid kinematic solutions (Figs 3b and c). Some shifts are observed in the kinematic solutions; however, they are mostly short-lived (less than 1d), not correlated across stations and are likely not tectonic in origin.

DISCUSSION

The lack of coseismic surface rupture and significant surface deformation may be attributed to the increased depth of the 2008 Achaia-Elia Earthquake. The initial focal depth estimates varied significantly from 5 to 38 km (table 2 in Ganas *et al.* 2009); however, the hypocentre depth was subsequently relocated with results between 18 and 22 km (Gallovič *et al.* 2009; Ganas *et al.* 2009; Konstantinou *et al.* 2009). Since very few relocated aftershocks were below 25 km (Ganas *et al.* 2009; Konstantinou *et al.* 2009), 25 km is probably the lower limit of the base of the seismogenic zone.

To test whether the increased depth can explain the coseismic surface deformation deficit, we develop a series of uniform-slip vertically dipping dextral fault models with different burial depths using the Okada (1992) dislocation model. We fix seismic moment $M_0 = 4.6 \times 10^{18}$ Nm (determined by gCMT), fault length $l = 25$ km as identified by early aftershocks (see fault surface trace in Fig. 3a), fault bottom at $h = 25$ km depth and average crustal rigidity $G = 3 \times 10^{10}$ Pa. We then determine the average slip $\bar{D}$ required for an event occurring below a burial depth b, by

$$\bar{D} = \frac{M_0}{Gl(h-b)}, \tag{3}$$

where $h - b$ represents the fault width w. The horizontal surface displacements along the line bisecting and normal to the fault trace for each model are calculated and plotted in the burial depth and fault normal distance space (solid curves in Fig. 4c). Though a trade-off between b and $\bar{D}$ is necessary to maintain constant M_0, deeper burial requires lesser surface deformation. The horizontal surface deformation normally bisecting a fault ranges from almost 5 cm at 2 km burial to a little more than 1 cm at 10 km burial depth. Considering the fault length and allowing a generous bottom depth (25 km), a burial depth to 10 km is unlikely as it would create an unnecessarily large $l : w$ aspect ratio. Alternatively, a more

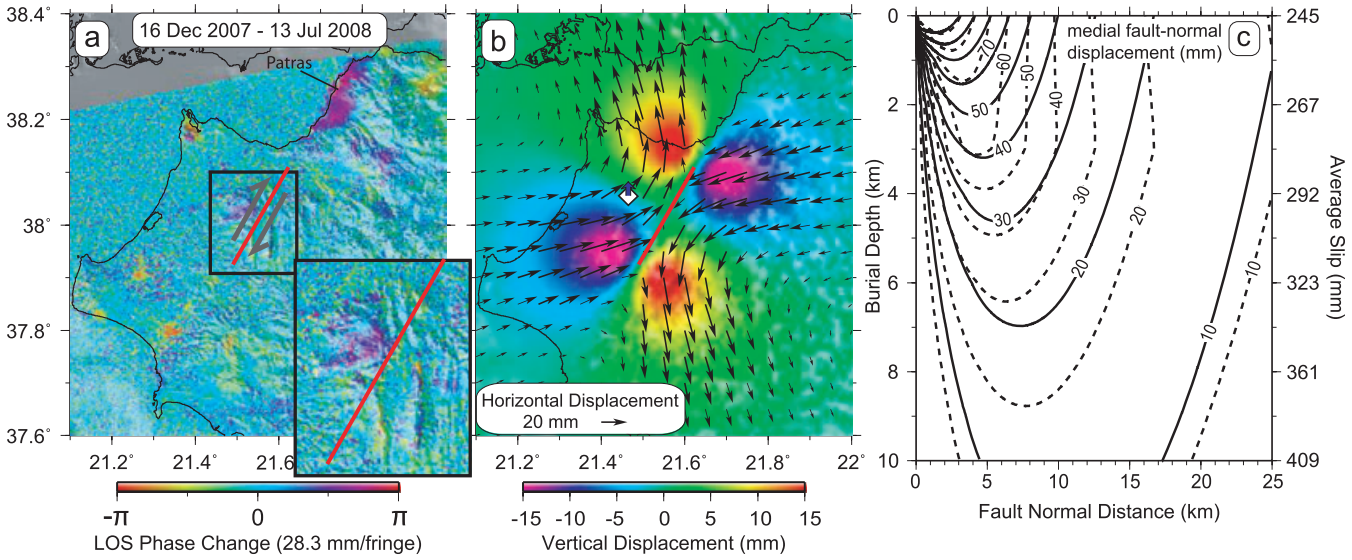

Figure 4. (a) The highly decorrelated ENVISAT ascending interferogram encompassing the 2008 Achaia-Elia Earthquake between 2007 December 16 and 2008 July 13. The colour shows the line-of-sight (LOS) motion away from the satellite with 28.3 mm fringe^{-1}. Red line is the same surface projection of the fault as Fig. 3(a). The inset is a blow-up of the near-fault region and shows increased coherence. (b) The horizontal (black arrows) and vertical (colours) displacements as expected from a dextral fault ($M_0 = 4.6 \times 10^{18}$ Nm) buried at 5 km depth in a homogeneous half-space ($G = 30$ GPa) with both length and bottom depth of 25 km. White diamond shows the location of NOANET continuous station RLS. Blue arrow indicates the 7.26 ± 0.28 mm northward motion of RLS during the earthquake (Ganas *et al.* 2009). (c) Predicted horizontal displacement (mm) normally bisecting the fault trace as described in (b) but with variable burial depth and average slip corresponding to $M_0 = 4.6 \times 10^{18}$ Nm. Homogeneous Okada half space models show in solid curves; two-layer continuum models show in dashed lines.

appropriate $b \sim 5$ km corresponding to the shallow extent of aftershocks to ∼4 km (Ganas *et al.* 2009). At $b = 5$ km, the predicted horizontal displacement is >2 cm between 3 and 13 km from the fault (Fig. 4c), while vertical deformation would be highly variable but with cross-fault differentials of near 3 cm (Fig. 4b). Such predicted displacements should be readily observable from InSAR. The only continuous GPS station running nearby during the 2008 Achaia-Elia Earthquake is the NOANET station RLS (Ganas *et al.* 2009), located ∼10 km away from the projected fault trace (Fig. 4b). A northward motion of 7.3 ± 0.3 mm was recorded at RLS (Ganas *et al.* 2009), much less than ∼20 mm that should be expected from a transform fault buried at 5 km depth (Figs 4b and c). The burial depth and downdip extent of the fault within a homogeneous elastic earth cannot explain the observed small surface deformation. Therefore, we argue that the compositionally weak, ∼3 km thick flysch layer acts as a near-surface decoupling agent that isolates subsurface deformation from the surface.

Flysch is a sequence of syn-orogenic deep-marine terrigenous-clastic deposits (van Hinsbergen *et al.* 2005). The flysch deposits in NW Peloponnese were accumulated on top of the pre-orogenic Triassic to Eocene carbonates in the Gavrovo-Tripolitza and Ionian foreland basins mainly in the Oligocene during the overthrusting course of the Pindos and Gavrovo-Tripolitza nappes onto the Ionian zone caused by the collision-subduction between the Apulian and Eurasian plates (Kamberis *et al.* 2000; Sotiropoulos *et al.* 2003; 2005; van Hinsbergen *et al.* 2005). The average thickness of the flysch deposits is estimated to be approximately 3000 m from seismic and borehole measurements (Kamberis *et al.* 2005). A portion of the Gavrovo-Tripolitza flysch is exposed in the middle part of the 2008 Achaia-Elia Earthquake region; while most of the flysch is covered by variously thick Pliocene-Quaternary sediments in the extensional basins rather than exposed at surface (Fig. 1b).

Flysch is characterized by rhythmic alternations of sandstone and pelitic layers of varying rock strength (Marinos & Hoek 2001); however, it is typically weak and compliant with $G \leq 5$ GPa (estimated from Marinos & Hoek 2001), much lower than carbonates, or granitic crust ∼20–30 GPa (e.g. Carmichael 1982). To understand whether the reduced rigidity alone can explain the lack of coseismic surface deformation, we employ an elastic model that has a 3-km thick surface layer with reduced rigidity ($G = 5$ GPa representing the flysch layer) over a stronger half-space ($G = 30$ GPa representing carbonates, or typical granitic crust) using Fortran programs EDGRN/EDCMP (Wang *et al.* 2003). Compared with homogeneous elastic models having the same fault parameters, the two-layer models allow for increased coseismic surface deformation (dashed curves in Fig. 4c). Thus, we conclude a detachment between the seismogenic crust and the flysch layer would best explain the lack of significant observed surface deformation.

With lower overall stress, the compliant flysch may allow for an essentially decoupled cap and hence lateral coseismic slip in the carbonates will not necessarily propagate through the flysch layer. A clear correlation between the strength of the geological formations and the existence of surface rupture was observed for the 1980 M_s 6.9 Irpinia normal earthquake in southern Apennines, Italy, where the surface faulting cut through carbonate platform rocks and was absent in the presence of thick flysch (Lyon-Caen *et al.* 1988; Bernard & Zollo 1989). Similarly, the detached surface layer may prohibit propagation of coseismic deformation to the surface as well. Strain in the flysch might be released independently by interseismic ductile deformation similar to that proposed by Fialko *et al.* (2005) for 2004 M_W 6.5 Bam earthquake in Iran, or fail in subsequent, smaller earthquakes.

Not only did the 2008 Achaia-Elia Earthquake have little discernable coseismic deformation, it had no perceptible early post-seismic surface deformation from our GPS analyses. The most likely and potentially substantial candidate for fault-related deformation in the months that follow the main shock is afterslip–aseismic slip

driven by a stress perturbation that builds as coseismic rupture is arrested within the upper 4–5 km velocity-strengthening region (Marone *et al.* 1991). Afterslip is observed to exist in regions of coseismic slip deficit and is at times comparable or larger in magnitude than coseismic slip for mature transform faults, which may have thick unconsolidated gouge zones at shallow depths, or faults overlain by poorly consolidated sediments (Marone *et al.* 1991; Marone 1998). The causal relation between unconsolidated fault gouge and afterslip suggests the 2008 Achaia-Elia Earthquake probably ruptured an immature fault without significant fault gouge that could favour afterslip. Instead, we suggest that the event had near complete coseismic slip along the seismogenically favourable fault at depth, but was unable to transmit significant stress to the potentially detached overriding flysch layer, making it unlikely to sustain any afterslip.

The 2008 Achaia-Elia Earthquake is the largest, but not the first strike-slip event in NW Peloponnese in recent history. Over 30 additional dominantly strike-slip crustal earthquakes with $M_W > 4$ have been identified between 1965 and 2009 in NW Peloponnese and surrounding regions from published reports and earthquake catalogues (compiled in Ganas *et al.* 2009, Fig. 5). A diffuse series of NE–SW trending dextral transform faults subparallel to the southern branch of CTF can be interpreted according to the distribution and focal mechanisms of these earthquakes. The major transform fault on which the 2008 Achaia-Elia Earthquake occurred extends at least 40-km long crossing NW Peloponnese and might connect with the

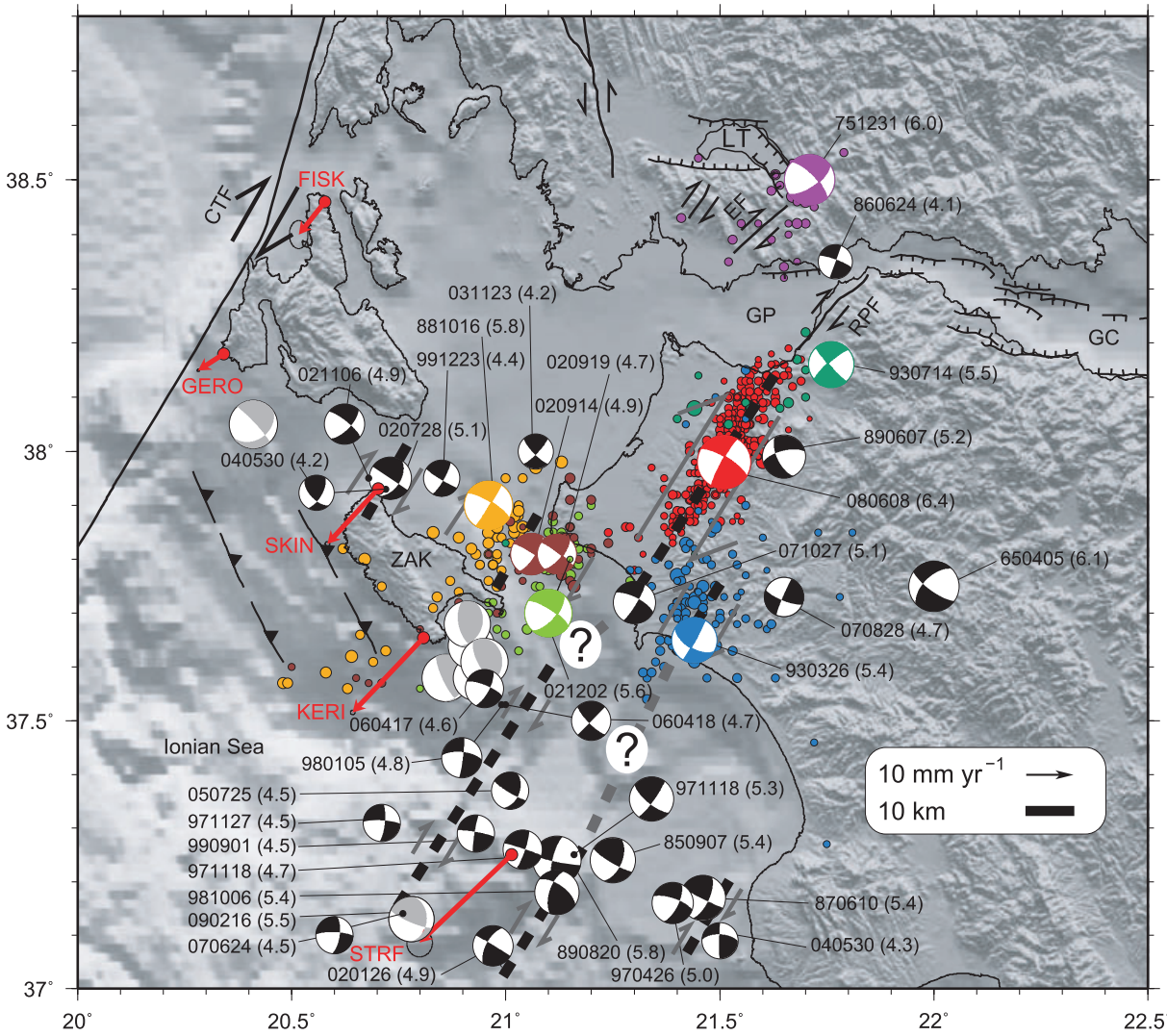

Figure 5. $M_W > 4$ strike-slip focal mechanisms in NW Peloponnese and surrounding regions. The seismic activity identifies a diffuse NE–SW trending transform fault zone in the crust (dark grey arrows and thick dash lines). Most fault planes are solutions combined from gCMT 1976–2009 and European-Mediterranean Regional CMT (RCMT) 1997–2009 (http://www.bo.ingv.it/RCMT). Higher quality solution is used if the same event exists in both; gCMT solution is used if the quality flags are the same. Benetatos *et al.* (2004) (for events 650 405, 850 907, 870 610, 890 820 and 930 714), Kiratzi *et al.* (2008) (for event 751 231) and Hatzfeld *et al.* (1990) (for event 860 624) are used as supplementary for missing events or events with low solution quality. Thrust earthquakes $M_W \geq 5.5$ in gCMT catalogue are also plotted for reference. Event locations (beach-balls) and 10-day aftershocks (circles) differentiated by colours are taken from Papanastassiou *et al.* (2001) for earthquakes in 1950–2000 and from the National Observatory of Athens catalogue (http://www.gein.noa.gr) after 2000. Faults are compiled from Ferentinos *et al.* (1985), Louvari *et al.* (1999), Flotté *et al.* (2005), Lagios *et al.* (2007), Kiratzi *et al.* (2008) and Bell *et al.* (2008). Red arrows show the horizontal velocities of GPS sites along the West Hellenic Arc during 1995–2001 relative to Eurasia (Hollenstein *et al.* 2006). GC, Gulf of Corinth; GP, Gulf of Patras; ZAK, Zakynthos Island; CTF, Cephalonia Transform Fault; RPF, Rion-Patras Fault; EF, Evinos Fault; LT, Lake Trichonis.

recently active Rion-Patras fault described by Flotté *et al.* (2005) to the north (Fig. 5). To the south, its extension likely continues further south for another 40 km into the Ionian Sea (Fig. 5). The dextral sense of motion on the major transform fault is widely accepted, however identification of fault and auxiliary planes was not clear for some events including 881016 (Kyllini) and 021202 (Vartholomio) earthquakes in the Zakynthos Channel and 930926 (Pyrgos) earthquake. The NE–SW trending 10-day aftershocks and the NE–SW differential shear motion shown by the continuous GPS sites along the West Hellenic Arc (Hollenstein *et al.* 2006, Fig. 5) suggest a dextral mechanism for each of the recorded events. The small, but widely spread, transform zone in the Zakynthos Channel is most likely restricted by a number of thrust events to the south and a possible more-rigid block to the north, as evidenced by low-seismicity rates (e.g. Hatzfeld *et al.* 1990). A similar wide spread transform zone is also observed in the Ionian Sea. The connection of the Ionian transform zone with the Pyrgos (930926) transform fault is not currently evident with the possibilities that either continuity between them or discontinuity by another small more-rigid block may exist. The 751231 earthquake near Lake Trichonis is likely a dextral slip event related to the Evinos fault just south of it. The newly recognized dextral shear zone had increasing activity over the past 30 yr and is potentially beginning to accommodate dextral shear between the Apulian and Aegean plates, similarly to the CTF.

Outside of some limited historical evidence of damaging events near Patras approximately 200 yr ago (Simopoulos 1985; Stiros 1995; Ambraseys & Jackson 1997), little is known about the earthquake potential and seismic hazard in the region. Hence, identification of the diffuse dextral shear zone that includes the 2008 event helps illuminate the internal deformation of the area. It is now evident that Patras, centrally located between this shear zone and the rapidly extending GC, has significant seismic hazard. Because the rates of deformation and historic activity are poorly constrained, more effort is necessary to evaluate the long-term recurrence and near-term potential of a moderate to large transform earthquakes near Patras.

CONCLUSIONS

We identified the 2008 June 8, M_W 6.4 Achaia-Elia Earthquake to have a highly energetic rupture with teleseismic M_e between 6.8 and 7.2. Such large energy release is highly suggestive of a near order-of-magnitude increase in stress-drop over the global average. Field investigation of GPS and analyses of InSAR images identify neither significant afterslip nor coseismic surface deformation, respectively. The contrasting increased shaking and lack of surface deformation can be explained by the existence of a thick and mechanically weak flysch layer covering the earthquake region that disassociates high-energy initial fault slip from the surface. The 2008 June 8, earthquake together with numerous smaller strike-slip events reveal an immature NE–SW trending dextral transform fault zone, which likely accommodates distributed shear between the central Ionian islands and NW Peloponnese.

ACKNOWLEDGMENTS

We thank T. H. Dixon and F. Amelung for thoughtful discussion and for use of the University of Miami's Geodesy lab for GPS data processing and SAR scene acquisition. F. Moschas and S. Lycourghiotis were invaluable during the field campaign. Images were created using GMT (Wessel & Smith 1991). The School of Earth and Atmospheric Sciences and the Georgia Tech Research Foundation supported this study. Some results are based on data and equipment provided by UNAVCO with support from NSF and NASA EAR-0735156.

REFERENCES

Allmann, B.P. & Shearer, P.M., 2009. Global variations of stress drop for moderate to large earthquakes, *J. geophys. Res.,* **114,** B01310, doi:10.1029/2008JB005821.

Ambraseys, N.N. & Jackson, J.A., 1997. Seismicity and strain in the Gulf of Corinth (Greece) since 1694, *J. Earthq. Eng.,* **1**(3), 433–474, doi:10.1080/13632469708962374.

Avallone, A. *et al*., 2004. Analysis of eleven years of deformation measured by GPS in the Corinth Rift Laboratory area, *C. R. Geosci.,* **336,** 301–311, doi:10.1016/j.crte.2003.12.007.

Bell, R.E., McNeill, L.C., Bull, J.M. & Henstock, T.J., 2008. Evolution of the western Gulf of Corinth, *Bull. geol. Soc. Am.,* **120,** 156–178, doi:10.1130/B26212.1.

Benetatos, C., Kiratzi, A., Papazachos, C. & Karakaisis, G., 2004. Focal mechanisms of shallow and intermediate depth earthquakes along the Hellenic Arc, *J. Geodyn.,* **37**(2), 253–296, doi:10.1016/j.jog.2004.02.002.

Bernard, P. & Zollo, A., 1989. The Irpinia (Italy) 1980 Earthquake: detailed analysis of a complex normal faulting, *J. geophys. Res.,* **94**(B2), 1631–1647.

Briole, P. *et al*., 2008. Multidisciplinary study of the June 8, 2008, M_W = 6.4 Andravida Earthquake. 31st General Assembly, European Seismol. Commission (Abstract).

Carmichael, R.S., 1982. *CRC Handbook of Physical Properties of Rocks,* Vol. 2, CRC Press, Boca Raton, Florida.

Choy, G.L. & Boatwright, J.L., 1995. Global patterns of radiated seismic energy and apparent stress, *J. geophys. Res.,* **100**(B9), 18 205–18 228.

Dewey, J.W., Choy, G., Presgrave, B., Sipkin, S., Tarr, A.C., Benz, H., Earle, P. & Wald, D., 2007. Seismicity associated with the Sumatra–Andaman islands earthquake of 26 December 2004, *Bull. seism. Soc. Am.,* **97**(1A), S25–S42, doi:10.1785/0120050626.

Doutsos, T. & Kokkalas, S., 2001. Stress and deformation patterns in the Aegean region, *J. Struct. Geol.,* **23,** 455–472, doi:10.1016/S0191-8141(00)00119-X.

Ekström, G., Dziewonski, A.M., Maternovskaya, N.N. & Nettles, M., 2005. Global seismicity of 2003: centroid-moment-tensor solutions for 1087 earthquakes, *Phys. Earth planet. Inter.,* **148**(2–4), 327–351, doi:10.1016/j.pepi.2004.09.006.

Ferentinos, G., Brooks, M. & Doutsos, T., 1985. Quaternary tectonics in the Gulf of Patras, western Greece, *J. Struct. Geol.,* **7**(6), 713–717, doi:10.1016/0191-8141(85)90146-4.

Fernandes, R.M.S., Ambrosius, B.A.C., Noomen, R., Bastos, L., Wortel, M.J.R., Spakman, W. & Govers, R., 2003. The relative motion between Africa and Eurasia as derived from ITRF2000 and GPS data, *Geophys. Res. Lett.,* **30**(16), 1828, doi:10.1029/2003GL017089.

Fialko, Y., Sandwell, D., Simons, M. & Rosen, P., 2005. Three-dimensional deformation caused by the Bam, Iran, earthquake and the origin of shallow slip deficit, *Nature,* **435,** 295–299, doi:10.1038/nature03425.

Flotté, N., Sorel, D., Müller, C. & Tensi, J., 2005. Along strike changes in the structural evolution over a brittle detachment fault: example of the Pleistocene Corinth-Patras rift (Greece), *Tectonophysics,* **403,** 77–94, doi:10.1016/j.tecto.2005.03.015.

Gallovič, F., Zahradník, J., Křížová, D., Plicka, V., Sokos, E., Serpetsidaki, A. & Tselentis, G.-A., 2009. From earthquake centroid to spatial-temporal rupture evolution: M_W 6.3 Movri mountain earthquake, June 8, 2008, Greece, *Geophys. Res. Lett.,* **36,** L21310, doi:10.1029/2009GL040283.

Ganas, A. & Parsons, T., 2009. Three-dimensional model of Hellenic Arc deformation and origin of the Cretan uplift, *J. geophys. Res.,* **114,** B06404, doi:10.1029/2008JB005599.

Ganas, A., Serpelloni, E., Drakatos, G., Kolligri, M., Adamis, I., Tsimi, Ch. & Batsi, E., 2009. The M_W 6.4 Achaia-Elia (Western Greece) Earthquake of 8 June 2008: seismological, field, GPS observations and stress modeling, *J. Earthq. Eng.,* **13,** 1101–1124, doi:10.1080/13632460902933899.

Hatzfeld, D., Pedotti, G., Hatzidimitriou, P. & Makropoulos, K., 1990. The strain pattern in the western Hellenic Arc deduced from a microearthquake survey, *Geophys. J. Int.,* **101**(1), 181–202.

Herring, T.A., King, R.W. & McClusky, S.C., 2008. *Introduction to GAMIT/GLOBK, Release 10.3,* Mass. Inst. of Techonol., Cambridge, USA.

Hollenstein, Ch., Geiger, A., Kahle, H.-G. & Veis, G., 2006. CGPS time-series and trajectories of crustal motion along the West Hellenic Arc, *Geophys. J. Int.,* **164**(1), 182–191, doi:10.1111/j.1365-246X.2005.02804.x.

Hollenstein, Ch., Muller, M.D., Geiger, A. & Kahle, H.-G., 2008. Crustal motion and deformation in Greece from a decade of GPS measurements, 1993–2003, *Tectonophysics,* **449,** 17–40, doi:10.1016/j.tecto.2007.12.006.

Kamberis, E., Pavlopoulos, A., Tsaila-Monopolis, S., Sotiropoulos, S. & Ioakim, C., 2005. Paleogene deep-water sedimentation and paleogeography of foreland basins in the NW Peloponnese (Greece), *Geologica Carpathica,* **56**(6), 503–515.

Kamberis, E., Sotiropoulos, S., Aximniotou, O., Tsaila-Monopoli, S. & Ioakim, C., 2000. Late Cenozoic deformation of the Gavrovo and Ionian zones in NW Peloponnesos (Western Greece), *Ann. Geofis.,* **43**(5), 905–919.

Kiratzi, A. *et al*., 2008. The April 2007 earthquake swarm near Lake Trichonis and implications for active tectonics in western Greece, *Tectonophysics,* **452,** 51–65, doi:10.1016/j.tecto.2008.02.009.

Konstantinou, K.I., Melis, N.S., Lee, S.-J., Evangelidis, C.P. & Boukouras, K., 2009. Rupture process and aftershocks relocation of the 8 June 2008 M_W 6.4 earthquake in northwest Peloponnese, western Greece, *Bull. seism. Soc. Am.,* **99**(6), 3374–3389, doi:10.1785/0120080301.

Kreemer, C. & Chamot-Rooke, N., 2004. Contemporary kinematics of the southern Aegean and the Mediterranean Ridge, *Geophys. J. Int.,* **157**(3), 1377–1392, doi:10.1111/j.1365-246X.2004.02270.x.

Lagios, E., Sakkas, V., Papadimitriou, P., Parcharidis, I., Damiata, B.N., Chousianitis, K. & Vassilopoulou, S., 2007. Crustal deformation in the Central Ionian Islands (Greece): results from DGPS and DInSAR analyses (1995–2006), *Tectonophysics,* **444,** 119–145, doi:10.1016/j.tecto.2007.08.018.

Le Pichon, X., Chamot-Rooke, N., Lallemant, S., Noomen, R. & Veis, G., 1995. Geodetic determination of the kinematics of central Greece with respect to Europe: implications for eastern Mediterranean tectonics, *J. geophys. Res.,* **100**(B7), 12675–12690.

Louvari, E., Kiratzi, A.A. & Papazachos, B.C., 1999. The Cephalonia transform fault and its extension to western Lefkada Island (Greece), *Tectonophysics,* **308,** 223–236, doi:10.1016/S0040-1951(99)00078-5.

Lyon-Caen, H. *et al*., 1988. The 1986 Kalamata (South Peloponnesus) earthquake: detailed study of a normal fault, evidences for east-west extension in the Hellenic Arc, *J. geophys. Res.,* **93**(B12), 14 967–15 000.

Margaris, B. *et al*., 2010. The 8 June 2008 M_W 6.5 Achaia-Elia, Greece earthquake: source characteristics, ground motions and ground failure, *Earthq. Spectra,* **26,** 399–424, doi:10.1193/1.3353626.

Marinos, P. & Hoek, E., 2001. Estimating the geotechnical properties of heterogeneous rock masses such as flysch, *Bull. Eng. Geol. Environ.,* **60,** 85–92, doi:10.1007/s100640000090.

Marone, C., 1998. Laboratory-derived friction laws and their application to seismic faulting, *Annu. Rev. Earth planet. Sci.,* **26,** 643–696, doi:10.1146/annurev.earth.26.1.643.

Marone, C.J., Scholz, C.H. & Bilham, R., 1991. On the mechanics of earthquake afterslip, *J. geophys. Res.,* **96**(B5), 8441–8452, doi:10.1029/91JB00275.

McClusky, S., *et al*., 2000. Global Positioning System constraints on plate kinematics and dynamics in the eastern Mediterranean and Caucasus, *J. geophys. Res.,* **105**(B3), 5695–5719.

Newman, A.V. & Convers, J.A., 2010. Convers, A rapid high-frequency energy-duration discriminant for very large and tsunami earthquakes, *Geophys. Res. Lett.,* submitted.

Newman, A.V. & Okal, E.A., 1998. Teleseismic estimates of radiated seismic energy: the E/M_0 discriminant for tsunami earthquakes, *J. geophys. Res.,* **103**(B11), 26 885–26 898.

Okada, Y., 1992. Internal deformation due to shear and tensile faults in a half-space. *Bull. seism. Soc. Am.,* **82**(2), 1018–1040.

Papanastassiou, D., Latoussakis, J. & Stavrakakis, G., 2001. A revised catalogue of earthquakes in the broader area of Greece for the period 1950–2000, in *Proceedings of the 9th Int. Congr. Geol. Soc. Greece, Athens, Bull. Geol. Soc.,* Greece, **XXXIV/4,** 1563–1566.

Reilinger, R. *et al*., 2006. GPS constraints on continental deformation in the Africa-Arabia-Eurasia continental collision zone and implications for the dynamics of plate interactions, *J. geophys. Res.,* **111,** B05411, doi:10.1029/2005JB004051.

Rosen, P.A., Henley, S., Peltzer, G. & Simons, M., 2004. Updated repeat orbit interferometry package released, *EOS, Trans. Am. geophys. Un.,* **85**(5), 47, doi:10.1029/2004EO050004.

Simopoulos, K., 1985. *Foreign Travellers in Greece* (in Greek), 5th edn, Vol. 3, Stachy, Athens, 582pp.

Sotiropoulos, S., Kamberis, E., Triantaphyllou, M.V. & Doutsos, T., 2003. Thrust sequences in the central part of the external Hellenides, *Geol. Mag.,* **140**(6), 661–668, doi:10.1017/S0016756803008367.

Stein, S. & Wysession, M., 2003. *An Introduction to Seismology, Earthquakes and Earth Structure,* pp. 1–498. Blackwell Publishing, Berlin, Germany.

Stiros, S.C., 1995. Archaeological evidence of antiseismic constructions in antiquity, *Ann. Geofis.,* **38**(5–6), 725–736.

Stiros, S.C., Pirazzoli, P.A., Laborel, J. & Laborel-Deguen, F., 1994. The 1953 earthquake in Cephalonia (Western Hellenic arc): coastal uplift and halotectonic faulting, *Geophys. J. Int.,* **117,** 834–849.

van Hinsbergen, D.J.J., van der Meer, D.G., Zachariasse, W.J. & Meulenkamp, J.E., 2006. Deformation of western Greece during Neogene clockwise rotation and collision with Apulia, *Int. J. Earth Sci.,* **95**(3), 463–490, doi:10.1007/s00531-005-0047-5.

van Hinsbergen, D.J.J., Zachariasse, W.J., Wortel, M.J.R. & Meulenkamp, J.E., 2005. Underthrusting and exhumation: a comparison between the external Hellenides and the 'hot' Cycladic and 'cold' South Aegean core complexes (Greece), *Tectonics,* **24,** TC2011, doi:10.1029/2004TC001692.

Wang, R., Lorenzo-Martín, F. & Roth, F., 2003. Computation of deformation induced by earthquakes in a multi-layered elastic crust—FORTRAN programs EDGRN/EDCMP, *Comput. Geosci.,* **29**(2), 195–207, doi:10.1016/S0098-3004(02)00111-5.

Weinstein, S.A. & Okal, E.A., 2005. The mantle wave magnitude M_m and the slowness parameter Θ: five years of real-time use in the context of tsunami warning, *Bull. seism. Soc. Am.,* **95**(3), 779–799, doi:10.1785/0120040112.

Wessel, P. & Smith, W.H.F., 1991. Free software helps map and display data, *EOS, Trans. Am. geophys. Un.,* **72,** 441.

Zumberge, J.F., Heflin, M.B., Jefferson, D.C., Watkins, M.M. & Webb, F.H., 1997. Precise point positioning for the efficient and robust analysis of GPS data from large networks, *J. geophys. Res.,* **102**(B3), 5005–5017.